

# Tunable Toxicity of Bufadienolides is Regulated through a Configuration Inversion Catalyzed by a Short-Chain Dehydrogenase/Reductase

Ge Ye<sup>+</sup>,<sup>[a]</sup> Weihuan Huang<sup>+</sup>,<sup>[e]</sup> Zeping Chen,<sup>[a]</sup> Hao Zhong,<sup>[a]</sup> Junhao Zhong,<sup>[a]</sup> Xiaoxin Guo,<sup>[a]</sup> Yuheng Huang,<sup>[a]</sup> Shruthi Kandalai,<sup>[b, c]</sup> Xiaozhuang Zhou,<sup>[b, c]</sup> Nan Zhang,<sup>[b, c]</sup> Yang Zhou,<sup>[f]</sup> Qingfei Zheng,<sup>\*[b, c, d]</sup> and Haiyan Tian<sup>\*[a]</sup>

Bufadienolides are toxic components widely found in amphibious toads that exhibit a wide range of biological activities. Guided by UPLC-QTOF-MS analysis, several 3-*epi*-bufadienolides with unique structures were isolated from the bile of the Asiatic toad, *Bufo gargarizans*. However, the enzymatic machinery of this epimerization in toads and its significance in chemical ecology remains poorly understood. Herein, we firstly compared the toxicities of two typical bufadienolides, bufalin (featuring a 14 $\beta$ -hydroxyl) and resibufogenin (containing a 14, 15-epoxy group), with their corresponding 3-*epi* isomers in a zebrafish model. The results of the toxicology assays showed that the ratio of maximum non-toxic concentrations of these two pairs

of compounds are 256 and 96 times, respectively, thereby indicating that 3-hydroxyl epimerization leads to a significant decrease in toxicity. Aiming to investigate the biotransformation of 3-*epi* bufadienolides in toads, we applied liver lysate to transform bufalin and found that it could stereoselectively catalyze the conversion of bufalin into its 3 $\alpha$ -hydroxyl epimer. Following this, we cloned and characterized a short-chain dehydrogenase/reductase, HSE-1, from the toad liver cDNA library and verified its 3( $\beta \rightarrow \alpha$ )-hydroxysteroid epimerization activity. To the best of our knowledge, this is the first hydroxyl epimerase identified from amphibians that regulates the toxicity of animal-derived natural products.

## Introduction

Bufadienolides are toxic components widely found in amphibious toads. They have been identified to serve as chemical defenses and exhibit a wide range of biological activities.<sup>[1]</sup> Among the reported bioactivities of bufadienolides, the anti-tumor effect has aroused a wide range of interest globally.<sup>[2]</sup> Previous studies have shown that bufadienolides exhibit potent cytotoxic activities against diverse cancer cell lines *in vitro*, with IC<sub>50</sub> values in the nanomolar range.<sup>[3]</sup> However, due to their inevitable cardiotoxicity, bufadienolides have not reached satisfactory efficacy *in vivo*, which has greatly hindered their

potential for drug development.<sup>[4]</sup> Although no clinical drugs have been developed from bufadienolides, toad venom and toad skin preparations, in which bufadienolides have been reported to be the main active ingredients, have diverse clinical applications in China, including inhibiting cancer growth, alleviating pain, and treating hepatitis.<sup>[5]</sup> For example, cinobufacini injections, water-soluble preparations made from the skin of *Bufo gargarizans*, have been widely applied in the clinic alongside chemotherapy for the treatment of various malignant cancers, with clinical data revealing that cinobufacini injections can significantly improve treatment efficacy and reduce side effects of chemotherapy.<sup>[6]</sup>

[a] G. Ye,<sup>+</sup> Z. Chen, H. Zhong, J. Zhong, X. Guo, Y. Huang, Prof. Dr. H. Tian  
Institute of Traditional Chinese Medicine and Natural Products, International Cooperative Laboratory of Traditional Chinese Medicine Modernization and Innovative Drug Development of Ministry of Education (MOE) of China  
College of Pharmacy, Jinan University  
855 Xingye East Avenue, 510632 Guangzhou (P. R. China)  
E-mail: thytian@jnu.edu.cn

[b] S. Kandalai, Dr. X. Zhou, Dr. N. Zhang, Prof. Dr. Q. Zheng  
Department of Radiation Oncology, College of Medicine  
The Ohio State University  
420 W. 12th Ave, 43210 Columbus, Ohio (USA)  
E-mail: Qingfei.Zheng@osumc.edu


[c] S. Kandalai, Dr. X. Zhou, Dr. N. Zhang, Prof. Dr. Q. Zheng  
Center for Cancer Metabolism  
James Comprehensive Cancer Center  
The Ohio State University,  
420 W. 12th Ave, 43210 Columbus, Ohio (USA)  
E-mail: Qingfei.Zheng@osumc.edu


[d] Prof. Dr. Q. Zheng  
Department of Biological Chemistry and Pharmacology, College of Medicine  
The Ohio State University,  
420 W. 12th Ave, 43210 Columbus, Ohio (USA)  
E-mail: Qingfei.Zheng@osumc.edu

[e] W. Huang<sup>+</sup>  
Key Laboratory of Regenerative Medicine  
Ministry of Education, Jinan University,  
601 West Huangpu Avenue, 510632 Guangzhou (P. R. China)

[f] Dr. Y. Zhou  
Guangzhou City Key Laboratory of Precision Chemical Drug Development  
College of Pharmacy, Jinan University  
855 Xingye East Avenue, 510632 Guangzhou (P. R. China)

[\*] These authors contributed equally to this work.

 Supporting information for this article is available on the WWW under <https://doi.org/10.1002/cbic.202200473>

 © 2022 The Authors. ChemBioChem published by Wiley-VCH GmbH. This is an open access article under the terms of the Creative Commons Attribution Non-Commercial NoDerivs License, which permits use and distribution in any medium, provided the original work is properly cited, the use is non-commercial and no modifications or adaptations are made.

Recently, we conducted a systematic chemical study on various parts of toads, including the venom, skin, and eggs, leading to the isolation of novel bufadienolides.<sup>[3a,7]</sup> In addition, the gallbladder and liver of toads have also been recorded in ancient Chinese medicinal books for the treatment of tracheitis and children's aphonia.<sup>[8]</sup> Following our previous research, we carried out comprehensive high-performance liquid chromatography-diode array detection (HPLC-DAD) analyses on different anatomical tissues of toads. Through these, we detected different levels of bufadienolides, with bile containing the highest abundance. As a result, we collected gallbladders from *Bufo gargarizans* and investigated the chemical composition of toad bile, which led to the isolation of several 3-hydroxyl isomerized bufadienolides (3-*epi* bufadienolides) (Figure 1). Further liquid chromatography–mass spectrometry (LC–MS) analysis revealed that 3-*epi* bufadienolides are distributed across various tissues (Figure S22 and Figure S23). Inspired by these findings, we compared the toxicities of 3-*epi* bufadienolides in a zebrafish model and found that epimerization significantly decreases toxicity. Additionally, we investigated the biosynthetic mechanism of 3-hydroxyl epimerization in toads. The results showed

that toad liver lysate can stereo-selectively catalyze the transformation of **6** into its 3 $\alpha$ -hydroxyl epimer (**1**). Furthermore, we cloned and characterized a short-chain dehydrogenase/reductase (named as HSE-1) from a toad liver complementary deoxyribonucleic acid (cDNA) library and verified its 3( $\beta$ → $\alpha$ )-hydroxysteroid epimerization activity utilizing human embryonic kidney 293T (HEK 293T) cells overexpressing this gene.

## Results

### Isolation of 3-*epi* bufadienolides from toad bile and their toxicities on zebrafish

Bufadienolides are characterized by a 2*H*-pyran-2-one moiety at the C-17 position of the steroidal core and typically show a maximum ultraviolet (UV) absorption band at 296 nm. Guided by HPLC-DAD, seven bufadienolides were isolated from the bile of *Bufo gargarizans*, four of which were 3-*epi* congeners (**1**–**4**, Figure 1A). Their structures were elucidated by nuclear magnetic resonance (NMR) and single crystal X-ray diffraction

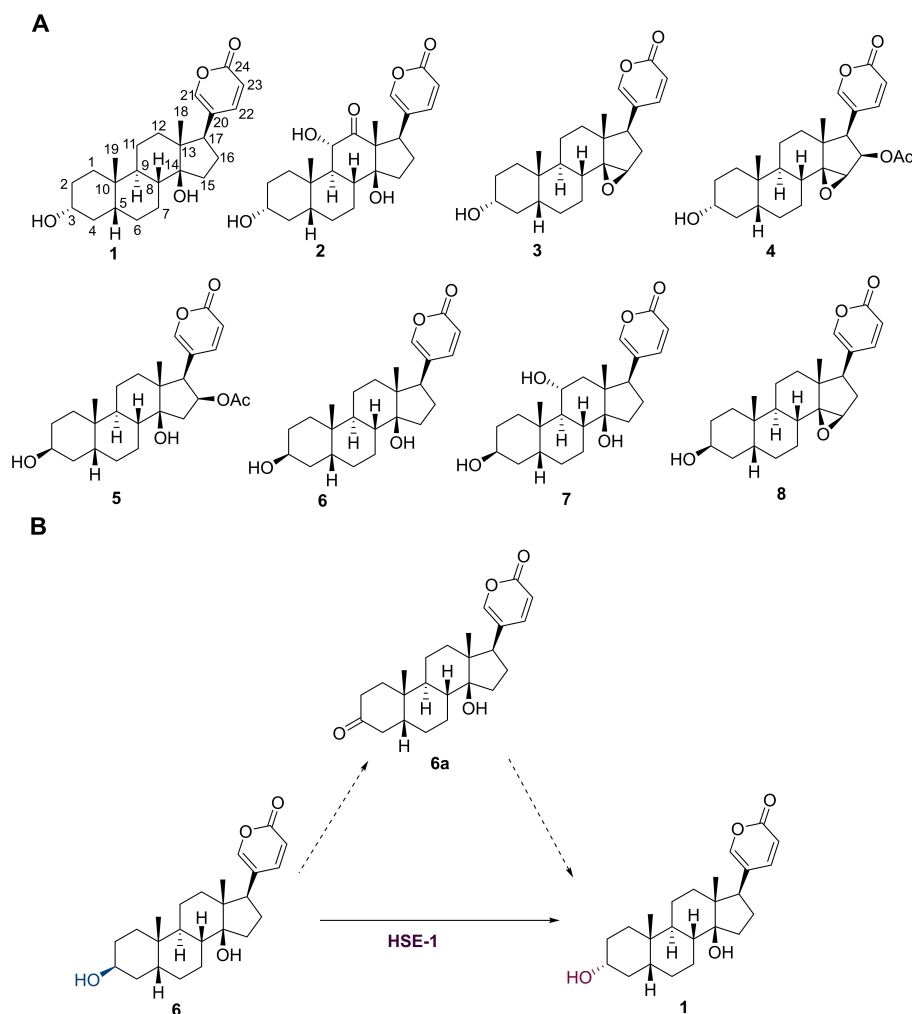


**Figure 1.** A) Bufadienolides from toad bile (**1**–**7**) and toad venom (**8**); B) Diagram illustrating the pathway of HSE-1-mediated conversion of bufalin (**6**) to 3-*epi* bufalin (**1**) through the formation of 3-ketone bufalin (**6a**) as an intermediate.

analyses (Supporting Information, Figure S1–10). Bufadienolides are known to be highly toxic, especially to the heart. Therefore, we compared the toxicities of two typical bufadienolides, bufalin (**6**), which features a 14 $\beta$ -hydroxyl, and resibufogenin (**8**), which is characterized by a 14, 15-epoxy group, with their corresponding 3-*epi* isomers (**1** and **3**) in a zebrafish model (Figure 2A). The results showed that compound **6** is more toxic than compound **8**, with lethal concentration 50 values (LC<sub>50</sub>s) of 1.18 ± 0.71 and 3.16 ± 1.2  $\mu$ M, respectively. In contrast, their maximum non-toxic concentrations (MNTCs) differed more significantly by a factor of 8, with MNTC values of 0.156 and 1.25  $\mu$ M, respectively. In addition, the toxicities of **6** and **8** with their corresponding 3-*epi* isomers revealed that the ratio of LC<sub>50</sub>s of the two pairs was 115 and 63, respectively, and that the ratio of MNTCs was 256 and 96, indicating the 3-hydroxyl epimerization causes a significant decrease in toxicity. Notably, although some concentrations between LC<sub>50</sub>s and MNTCs did not cause the death of the zebrafish, varying degrees of physiological toxicity, as noted by pericardial edema and curved tails, were observed (Figure 2B).

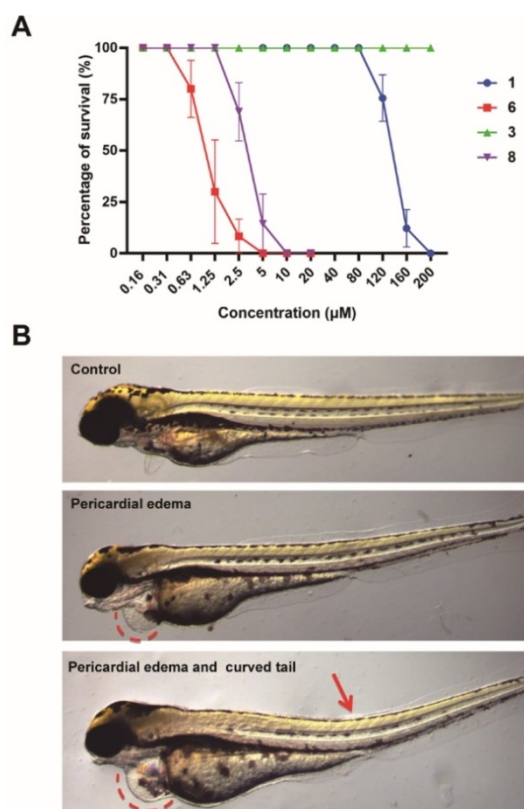


**Figure 2.** Toxic effects of compounds on embryonic development of zebrafish. A) Different concentrations of compounds **1**, **3**, **6**, and **8** exert differential effects on the survival of zebrafish embryos ( $n = 30$  for each group). B) Morphological changes in zebrafish embryos due to compound **6** (0.6  $\mu$ M) were observed, including pericardial edema and curved tail. The red dotted line and red arrow point to pericardial edema and curved tail, respectively.

### Catalytic activity of toad liver towards bufadienolides

As the liver produces bile before it is stored and concentrated in the gallbladder, we speculated that there might be enzymes in toad liver which could catalyze the transformation of bufadienolides into their 3-hydroxyl epimers. To confirm this speculation, we used toad liver lysates to transform a representative bufadienolide, bufalin (**6**), with the results showing that **6** was somewhat transformed into 3-*epi*-bufalin (**1**). In order to validate if this transformation is stereoselective, 3-*epi*-bufalin (**1**) was reacted with toad liver lysates in parallel, and this was not able to convert **1** back to **6**. As hydroxyl epimerization often has a ketone intermediate, we synthesized 3-ketone bufalin (**6a**) and incubated **6a** with toad liver lysates. This resulted in 3-ketone bufalin (**6a**) being somewhat transformed into 3-*epi* bufalin (**1**) (Figure 3). These experiments strongly suggest that the toad liver possess stereoselectivity for both oxidative and reductive reactions (Figure 1B).

### Bioinformatics analysis of candidate HSEs in toad liver transcriptome

Previous results indicated that short-chain dehydrogenases/reductases (SDRs) could catalyze the dehydrogenation of alcohols and the reduction of ketones.<sup>[9]</sup> Among the literature, two papers attracted our attention, with one reporting a human 3( $\alpha \rightarrow \beta$ )-hydroxysteroid epimerase (AF223225)<sup>[10]</sup> and the other

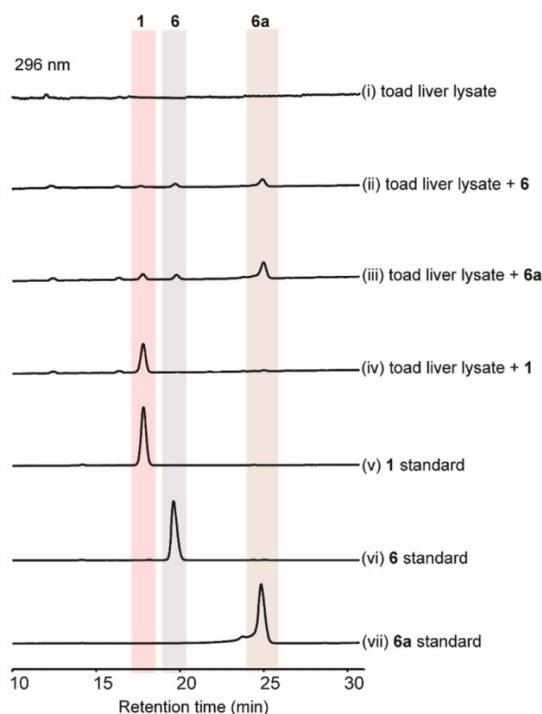


**Figure 3.** Identification of biotransformation products by HPLC. All the reactions were performed at 37 °C for 6 h: (i) toad liver lysate; (ii) toad liver lysate + 5  $\mu$ M **6**; (iii) toad liver lysate + 5  $\mu$ M **6a**; (iv) toad liver lysate + 5  $\mu$ M **1**; (v) **1** standard; (vi) **6** standard; (vii) **6a** standard.

reporting a biosynthetic pathway for 3-hydroxyl epimerization of bile acid in bacteria, which was catalyzed by two separate enzymes.<sup>[11]</sup> Because toads are more closely related to humans than bacteria, we chose the AF223225 encoded protein sequence as a query and performed blastP in the local transcriptome of a toad liver sample. From this bioinformatic search, 11 candidate homologs were identified that shared similarity to AF223225, with a minimum similarity of 50% (Supporting Information, Table S1). Among the 11 candidate genes *hse 1–11*, seven (*hse 1–7*) were successfully cloned from the cDNA library into a pcDNA3.1 (+) plasmid vector (Supporting Information, Figure S11–13).

### Determination of enzymatic activity of candidate HSE enzymes

To test their activities, we performed transient transfection and overexpressed genes *hse 1–7* in HEK 293T cells. Then, we incubated these 293T cells with the compounds **1**, **6**, and **6a**. HPLC-DAD analysis showed that 293T cells transfected with the toad *hse-1* gene produced new peaks that mimicked the typical UV absorption curve of bufadienolides, suggesting that HSE-1 can transform bufalin (**6**) into 3-ketone bufalin (**6a**) and 3 $\alpha$ -bufalin (**1**) (Figure 4A). Therefore, further analysis focused on activity of HSE-1, specifically. HPLC-DAD profiles showed that HSE-1 also catalyzed the reduction of 3-ketone bufalin (**6a**) to 3 $\alpha$ -bufalin (**1**) and a small amount of bufalin (**6**) (Figure 4B). It should be noted that the wild-type 293T cells have some ability to reduce the ketone intermediate **6a** into 3 $\alpha$ -bufalin (**1**), which may be attributed to the widely distributed aldo-keto reductases (AKRs) in mammalian cells.<sup>[12]</sup> HPLC-DAD profiles showed that HSE-1 was not able to catalyze the transition of 3 $\alpha$ -bufalin (**1**) to bufalin (**6**) or 3-ketone bufalin (**6a**) (Figure 4C). In order to further confirm that HSE-1 can reduce ketones, we carried out time gradient experiments and used different concentrations of 3-ketone bufalin (**6a**). The results showed that 293T cells transfected with *hse-1* had significantly stronger reduction function at the four timepoints of **6**, **8**, **10**, and **12** hours and preferred to reduce the ketone to an  $\alpha$  configuration (Supporting Information, Figure S17 and Figure S27).

Based on bioinformatics analysis, we noted that HSE-1 belongs to the SDR superfamily, which has a highly conserved nicotinamide cofactor binding site with the sequence motifs of TGX<sub>3</sub>GXG or TGX<sub>2</sub>GXG.<sup>[9]</sup> We then conducted site-directed mutagenesis to validate the catalytic function and mechanism of HSE-1. The Thr at position 35, Cys at position 37, and Asp at position 38 were all changed to Ala (Supporting Information, Table S5). An expression vector bearing the mutant sequence in parallel with *hse-1* and the blank vector were transfected into 293T cells and protein expression levels were evaluated by Western blot analysis. We found that the mutation greatly influenced the protein expression level and the catalytic activities of HSE-1 (Supporting Information, Figure S20 and S21). Given the relatively low biotransformation efficiency of HSE-1 in 293T cells, we speculate that there might be other ketoreduc-

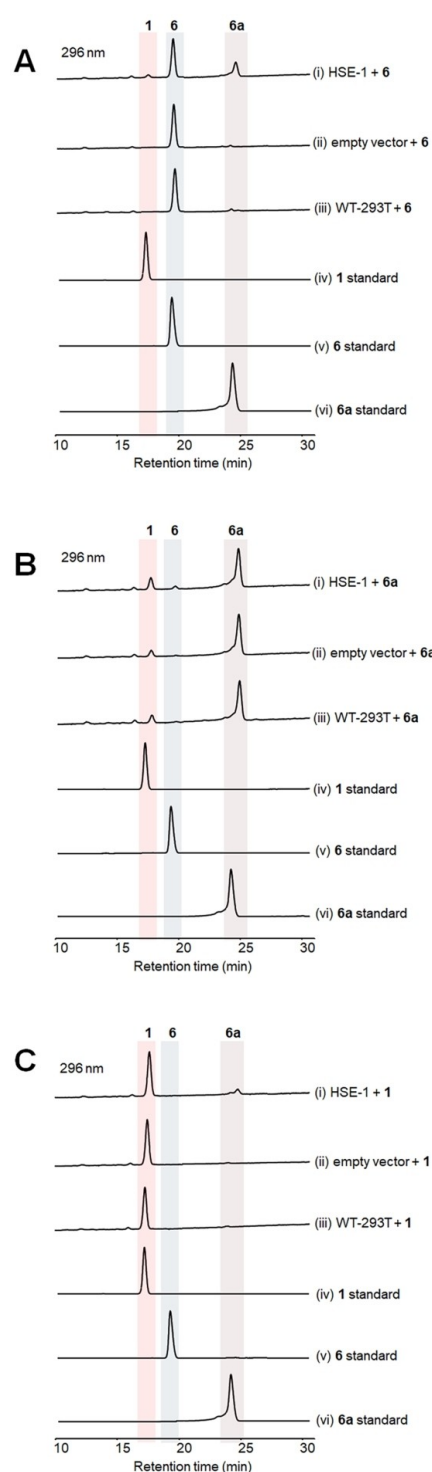


**Figure 4.** Identification of biotransformation products by HPLC. All the reactions were performed in living 293T cells at 37 °C for 6 h: A) biotransformation of 5  $\mu$ M bufalin (**6**) by HSE-1; B) biotransformation of 5  $\mu$ M 3-ketone bufalin (**6a**) by HSE-1; C) biotransformation of 5  $\mu$ M 3-epi bufalin (**1**) by HSE-1 (no reaction).

tases in the toad liver participating in this conversion process, especially during the second step (from **6a** to **1**).

## Multiple sequence alignment and phylogenetic analysis of HSE-1

To illustrate the unique catalytic activity of HSE-1 among SDRs, a phylogenetic tree was constructed through the multiple sequence alignment of 15 representative SDR candidates, 14 of which were selected with sequence similarity more than 50% and one from plants as a comparison (Supporting Information, Figure S22). The phylogenetic analysis revealed that the proteins with relatively high similarity to HSE-1 are from humans and other animal species. The highest similarity in sequence alignment between HSE-1 and the SDR candidates was found to be 59% with *Homo sapiens* RDH16, a retinol dehydrogenase (Supporting Information, Table S7).

## Discussion and Conclusion

The occurrence of steroid hydroxyl isomerization is closely related to their tunable toxicity in physiology. In particular, the hydroxyl isomerization at C-3 position of steroidal core often causes large changes in physiological function and biological activities.<sup>[10]</sup> For example, the steroid allo-pregnanolone (5 $\alpha$ -pregnane-3 $\alpha$ -ol-20-one) can modulate reproductive function, while iso-pregnanolone (5 $\alpha$ -pregnane-3 $\beta$ -ol-20-one) is ineffective and instead, has an effect on premenstrual syndrome.<sup>[13]</sup> Another example is the C-3 hydroxyl isomers of bile acids in human intestinal symbionts, which have weaker detergent activity and toxicity.<sup>[11]</sup> In this paper, the biosynthetic mechanism of C-3 hydroxyl isomerization of an important class of steroidal toxins, bufadienolides, has been elucidated for the first time. Our results indicate that HSE-1 possesses dual activities of oxidation and reduction, regulating the epimerization of bufadienolides into their 3-*epi* isomers. As shown in Figure 1B, the transformation is composed of two steps, the oxidation of 3 $\beta$ -hydroxyl into a ketone group, followed by a reduction of the ketone into 3 $\alpha$ -hydroxyl. Importantly, we transfected HEK 293T cells to investigate the enzymatic activity of HSE-1, directly indicating its function in living cells under natural conditions. Furthermore, we found that the toxicity of 3-*epi*-bufalin (**1**) was reduced by 256-fold compared with bufalin (**6**) in a zebrafish model, which is much more significant than our previous data regarding the inhibition ratio of these two compounds on sodium-potassium ATPase,<sup>[14]</sup> a well-established cardiotoxic target of bufadienolides. This indicates that hydroxyl epimeriza-

tion reduces the toxicities of bufadienolides through a complex mechanism. The toxicological experiments on zebrafish in this work served as a research model to study the activities of toad toxins on other aquatic animals, providing new insights into their elusive functions in chemical ecology. Moreover, since 3-*epi*-bufadienolides are widely distributed within toads, in multiple regions including the blood, kidneys, and heart, these compounds may possess special endogenous physiological roles, which require further investigation.

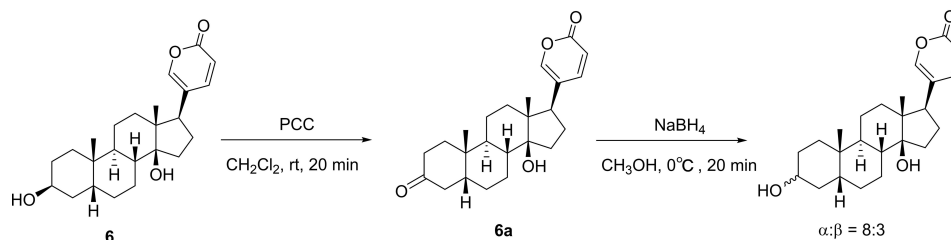
## Experimental Section

**Materials:** Adult *Bufo gargarizans* and toad gallbladders were provided by Lianyungang Toad Breeding Base in Jiangsu Province of China and authenticated by Dr. Haiyan Tian (Institute of Traditional Chinese Medicine & Natural Products, Jinan University, Guangzhou, People's Republic of China). *E. coli* strain DH5 $\alpha$  was preserved at  $-80^{\circ}\text{C}$  and 293T cells were preserved in liquid nitrogen in our laboratory.

**Extraction and isolation of bufadienolides from toad bile:** The toad gallbladders (707.6 g) were homogenized and extracted by 95% EtOH under ultrasonic condition four times ( $45^{\circ}\text{C}$ , 60 min each time). The combined EtOH extract was filtered and concentrated under reduced pressure to give a residue (59.1 g), which was suspended in 20% EtOH and subsequently partitioned by cyclohexane,  $\text{CH}_2\text{Cl}_2$ , and *n*-BuOH. The  $\text{CH}_2\text{Cl}_2$  fraction (5.0 g) was subjected to silica gel (200–300 mesh) and eluted with petroleum ether/acetone gradients (100:0, 100:1, 20:1, 10:1, 6:1, 4:1, 3:1, 2:1, 1:1, 0:1) to yield 14 sub-fractions (Fr. 1–Fr. 14). Fr.1 was further purified by preparative HPLC (MeOH/ $\text{H}_2\text{O}$ , 85%, flow rate 3 mL) to yield compound **3** (8.6 mg). Fr. 8 was separated by preparative HPLC (MeOH/ $\text{H}_2\text{O}$ , 65%, flow rate 3 mL) to yield compounds **1** (10.9 mg), **4** (9.0 mg), and **5** (6.4 mg). Fr. 9 was separated by preparative HPLC (MeOH/ $\text{H}_2\text{O}$ , 65%, flow rate 3 mL) to yield compounds **6** (5.5 mg) and **7** (4.8 mg). Compound **2** (1.2 mg) was obtained from Fr. 10 by preparative HPLC (MeOH/ $\text{H}_2\text{O}$ , 55%, flow rate 3 mL) and recrystallization. For the  $^1\text{H}$  and  $^{13}\text{C}$  NMR data of **1–6** and X-ray crystallography data of **7**, see Supporting Information.

## Synthesis of 3-ketone and 3 $\alpha$ -bufadienolides

**6** (45 mg, 0.12 mmol) and pyridinium chlorochromate (PCC, 50 mg, 0.23 mmol) were added to a flask and dissolved with  $\text{CH}_2\text{Cl}_2$  (5 mL). The mixture was stirred at room temperature and the reaction was monitored by TLC analysis. After 15 min, the mixture was distilled with water (10 mL). The organic layer was separated and washed with water ( $2 \times 10$  mL). The organic layer was dried with anhydrous sodium sulfate and the solvent was removed under reduced pressure to yield **6a** (30 mg, 0.08 mmol) (Scheme 1).



Scheme 1. Synthesis of **1** and **6a** by chemical methods.

**6a** (23 mg, 0.06 mmol) and sodium borohydride (3.2 mg, 0.09 mmol) were added to a flask and dissolved with MeOH (2 mL). The mixture was stirred in ice water and the reaction was monitored by TLC analysis. After 30 min, the mixture was distilled with water (10 mL). The organic layer was dried and concentrated under reduced pressure. The product was diluted with 5 mL of water and extracted with ethyl acetate (5 × 3 mL). The ethyl acetate extract was purified by preparative HPLC (Phenomenex column C4, MeOH-H<sub>2</sub>O, 7:3) to yield compounds **1** (8 mg, 0.02 mmol) and **6** (3 mg, 0.0077 mmol).

**8** (30 mg, 0.08 mmol) and pyridinium chlorochromate (PCC, 30 mg, 0.14 mmol) were added to a flask and dissolved with CH<sub>2</sub>Cl<sub>2</sub> (5 mL). The mixture was stirred at room temperature and the reaction was monitored by TLC analysis. After 15 min, the mixture was distilled with water (10 mL). The organic layer was separated and washed with water (2 × 10 mL). The organic layer was dried with anhydrous sodium sulfate and the solvent was removed under reduced pressure to yield **8a** (25 mg, 0.07 mmol) (Scheme 2).

**8a** (10 mg, 0.02 mmol) and sodium borohydride (4.0 mg, 0.11 mmol) were added to a flask and dissolved with MeOH (2 mL). The mixture was stirred in ice water and the reaction was monitored by TLC analysis. After 30 min, the mixture was distilled with water (10 mL). The organic layer was dried and concentrated under reduced pressure. The product was diluted with 5 mL of water and extracted with ethyl acetate (5 × 3 mL). The ethyl acetate extract was purified by preparative HPLC (Phenomenex column C4, MeOH-H<sub>2</sub>O, 7:3) to yield **3** (4 mg, 0.01 mmol) and **8** (2 mg, 0.005 mmol).

**Catalytic activity of toad liver towards bufadienolides:** The liver was dissected from *Bufo gargarizans*. Following a saline wash, 400 mg of liver was weighed, sliced, and submerged in 4 mL 1 × PBS. We set up two control groups, one without bufadienolides and the other with boiled liver. The three experimental groups included bufalin (**6**), 3-*epi* bufalin (**1**), and 3-ketone bufalin (**6a**) as substrates. The optimized final concentration of each substrate was 5 μM. Samples were incubated in a 37 °C shaker for 6 hours. After incubation, the samples were extracted with an equal volume ethyl acetate three times, before being dried and dissolved in 100 μL of methanol. Reaction products were resolved by high-performance liquid chromatography (HPLC) using Lux Cellulose-4 Chiral Column (5 μM, 4.6 × 250 mm, Phenomenex, USA) and detected at 296 nm.

**Bioinformatics analysis of HSE-1:** Fresh liver was dissected from *Bufo gargarizans* and immediately frozen on dry ice. Then, it was sent to Tsingke Biotechnology Co., Ltd., for transcriptome sequencing and cDNA library construction. Based on these sequences, a local nucleotide and protein database was established by Basic Local Alignment Search Tool (BLAST, ftp://ftp.ncbi.nlm.nih.gov/blast/executables/blast+/LATEST/). The protein sequence of human 3(α→β)-hydroxysteroid epimerase was downloaded from the NCBI database (http://www.ncbi.nlm.nih.gov) according to the Genbank number AF223225. We identified HSE-1 candidate genes

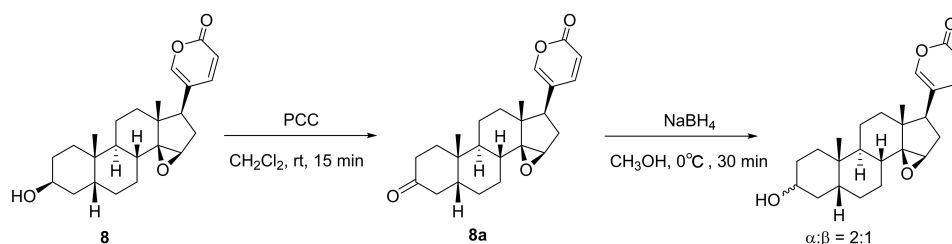
using the basic alignment sequence tool blastP with human 3(α→β)-hydroxysteroid epimerase (AF223225) as a query. Homologs of AF223225 in *Bufo gargarizans* liver transcriptome are shown in Supporting Information Table S1. The potential open reading frames (ORFs) of HSE-1 candidate genes were predicted using open reading frame finder (<https://www.ncbi.nlm.nih.gov/orffinder>). All primers used to amplify candidate genes are included in Supplemental Information Table S2.

**Cloning of HSE-1 and constructing the expression plasmid:** A total of 20 mg of fresh toad liver was weighted to extract total RNA by using MolPure® Cell/Tissue Total RNA Kit (Yeasen, China). Hifair® II 1st Strand cDNA Synthesis Kit (Yeasen, China) was used to synthesize the first strand cDNA (Bbg-cDNA). The ORF of HSE-1 was obtained using Bbg-cDNA as template and amplified by PrimeSTAR HS DNA Polymerase (TaKaRa Bio, Shiga, Japan) with primers designed according to the ORF of the full-length HSE-1 cDNA. The primer sequences that were used are shown in Supporting Information Table S3. The PCR cycling program was performed as follows: 94 °C for 10 min, then 30 cycles of 94 °C for 30 s, 55 °C for 30 s, 72 °C for 30 s, and a final extension at 72 °C for 10 min.

The fragment of HSE-1 and pcDNA3.1 (+) were double digested by HindIII (TransGen Biotech) and BamHI (TransGen Biotech). The target fragment was recycled after 1% agarose gel electrophoresis and linked by Ligation Mix at 16 °C overnight. Then, the recombinant plasmid was transferred to *E. coli* DH5α competent cells and the positive clones were screened by PCR using the primers 3(β→α)-HSE-F and 3(β→α)-HSE-R. Positive single colonies of transformed *E. coli* DH5α were transferred to overnight cultures [5 mL, lysogeny broth, ampicillin (100 μg/mL)]. Plasmid extraction was performed the next day and sent for sequencing.

**Sequence and phylogenetic analysis of HSE-1:** The ORF of HSE-1 was predicted using the ORF Finder program from NCBI (<https://www.ncbi.nlm.nih.gov/orffinder>). Protein sequences of short-chain dehydrogenases/reductases (SDRs) family from different species were downloaded from UniprotKB. We identified candidate genes for phylogenetic analysis using the basic alignment sequence tool blastP with HSE-1 as a query, considering the BLAST hits with more than 50% similarity as potential candidate genes. A phylogenetic tree was constructed by the neighbor joining method, with a bootstrap number set to 1000 replicates.

**Site-directed mutation:** The mutation sites of HSE-1 are shown in Table S5. The changes were from T to A, C to A, and D to A at positions 35, 37 and 38, respectively. The mutations at the corresponding sites were created by the overlap PCR method with the template plasmids containing the wild-type 3(β→α)-HSE gene. The primers are listed in Table S4. The PCR cycling program was performed as follows: 95 °C for 3 min, then 25 cycles of 95 °C for 25 s, 62 °C for 20 s and 72 °C for 40 s, and a final extension at 72 °C for 1 min. The gene fragments were digested with HindIII (TransGen Biotech) and BamHI (TransGen Biotech), then ligated to the pcDNA3.1 (+) vector. Ligation products were transformed in *E. coli*



**Scheme 2.** Synthesis of **3**, **8**, and **8a** by chemical methods.

Top 10, positive clones were screened, and plasmids were extracted and then sent for sequencing.

**Epimerase activity assays:** These experiments were conducted at the same conditions as liver lysate experiment above. The determination of the enzyme activity in intact 293T cells was done as follows: (1)  $4 \times 10^5$  293T cells were seeded and allowed to grow until reaching 60% confluence in supplemented DMEM media; (2) The pcDNA3.1(+)-HSE-1, pcDNA3.1(+)-HSE-1-T35A-C37A-D38A (site mutant) and pcDNA3.1(+) empty vector were transiently transfected into 293T cells with a Lipofectamine 2000 transfection reagent (Invitrogen). After 6 h, the medium was changed to fresh complete DMEM; (3) After 18 h, 5  $\mu$ M of the bufalin (6), 3-*epi* bufalin (1), or 3-ketone bufalin (6a) were added to 6-well plate and incubated at 37 °C for 6 h; (4) After the incubation, the samples were extracted with an equal volume of ethyl acetate three times, dried, and dissolved in 100  $\mu$ L methanol; (5) Reaction products were resolved by high-performance liquid chromatography (HPLC) using Lux Cellulose-4 (5  $\mu$ M, 4.6  $\times$  250 mm, Phenomenex, U.S.A) and detected by their UV absorption at 296 nm.

**Zebrafish embryo and larvae maintenance:** Adult AB strain zebrafish (*Danio rerio*) were obtained from College of Pharmacy, Jinan University (Guangzhou, China). Zebrafish adults were maintained in aerated 5 liter tanks at 26 °C, in a 10:14 hour light:dark cycle. In each mating setup, two females and one male fish were present. Embryos were collected within the first hour, washed, sorted, and transferred to Petri dishes filled with embryo water (0.2 g/L sea salt water). The zebrafish embryos were cultured at 28.5 °C for further experiments. All the animal protocols used in this study have been approved by Jinan University (Guangzhou, China).

**Toxicity experiments on zebrafish:** Healthy zebrafish larvae at 48 hours post-fertilization ( $n=30$  for each group) were selected and treated with a range of concentrations (0.16–200  $\mu$ M) of compounds 1, 3, 6, and 8 in 6-well plates. After 48-hour treatment, survival and pathological changes of the zebrafish larvae were observed under the stereomicroscope (Olympus SZX7). Results are from at least three independent experiments. The data were analyzed by Graph Pad Prism 7.0. Data were calculated to determine indices  $LC_{50}$ s and MNTCs.

## Acknowledgements

This research work was financially supported by the National Natural Science Foundation (No. 82173938), the National Natural Science Foundation of Guangdong Province, China (No. 2019A1515011489), the Guangzhou Science and Technology Plan (202002030219) for H. T. and the OSUCCC startup funds for Q. Z.

## Conflict of Interest

All authors declare that there is no potential conflict of interest include employment, consultancies, stock ownership, honoraria, paid expert testimony, patent applications/registrations, and grants or other funding.

## Data Availability Statement

The data that support the findings of this study are available from the corresponding author upon reasonable request.

**Keywords:** 3-*epi* bufadienolides · hydroxysteroid epimerization · short-chain dehydrogenase/reductase · toad liver · toxicity

- [1] a) H. Gao, R. Popescu, B. Kopp, Z. Wang, *Nat. Prod. Rep.* **2011**, *28*, 953–969; b) P. S. Steyn, F. R. van Heerden, *Nat. Prod. Rep.* **1998**, *15*, 397–413.
- [2] a) L. J. Deng, Y. Li, M. Qi, J. S. Liu, S. Wang, L. J. Hu, Y. H. Lei, R. W. Jiang, W. M. Chen, Q. Qi, H. Y. Tian, W. L. Han, B. J. Wu, J. X. Chen, W. C. Ye, D. M. Zhang, *Eur. J. Pharmacol.* **2020**, *887*, 173379; b) F. J. Li, J. H. Hu, X. Ren, C. M. Zhou, Q. Liu, Y. Q. Zhang, *Arch. Pharm.* **2021**, *354*, e2100060.
- [3] a) S. W. Zhou, J. Y. Quan, Z. W. Li, G. Ye, Z. Shang, Z. P. Chen, L. Wang, X. Y. Li, X. Q. Zhang, J. Li, J. S. Liu, H. Y. Tian, *J. Nat. Prod.* **2021**, *84*, 1425–1433; b) P. L. Wu, Y. L. Hsu, T. S. Wu, K. F. Bastow, K. H. Lee, *Org. Lett.* **2006**, *8*, 5207–5210; c) H. Shao, B. Li, H. Li, L. Gao, C. Zhang, H. Sheng, L. Zhu, *Molecules* **2022**, *27*, 51.
- [4] a) D. M. Zhang, J. S. Liu, L. J. Deng, M. F. Chen, A. Yiu, H. H. Cao, H. Y. Tian, K. P. Peng, H. Kurihara, J. X. Pan, W. C. Ye, *Carcinogenesis* **2013**, *34*, 1331–1342; b) L. J. Deng, Y. Li, M. Qi, J. S. Liu, S. Wang, L. J. Hu, Y. H. Lei, R. W. Jiang, W.-M. Chen, Q. Qi, H. Y. Tian, W. L. Han, B. J. Wu, J. X. Chen, W. C. Ye, D. M. Zhang, *Eur. J. Pharmacol.* **2020**, *887*, 173379.
- [5] W. L. Wei, J. J. Hou, X. Wang, Y. Yu, H. J. Li, Z. W. Li, Z. J. Feng, H. Qu, W. Y. Wu, D. A. Guo, *J. Ethnopharmacol.* **2019**, *237*, 215–235.
- [6] a) Z. Chen, X. F. Zhai, Y. H. Su, X. Y. Wan, J. Li, J. M. Xie, B. Gao, *Zhongxiyi Jiehe Xuebao* **2003**, *1*, 184–186; b) Y. Xu, D. Han, F. C. Feng, Z. C. Wang, C. Gu, W. P. Peng, H. L. He, X. M. Zhou, *Zhongguo Zhongyao Zazhi* **2019**, *44*, 4728–4737; c) J. Xu, S. S. Qian, Y. G. Chen, D. Y. Li, Q. Yan, *Zhongguo Zhongyao Zazhi* **2019**, *44*, 2627–2636.
- [7] a) H. Y. Tian, L. Wang, X. Q. Zhang, Y. Wang, D. M. Zhang, R. W. Jiang, Z. Liu, J. S. Liu, Y. L. Li, W. C. Ye, *Chem. Eur. J.* **2010**, *16*, 10989–10993; b) H. Y. Tian, L. J. Ruan, T. Yu, Q. F. Zheng, N. H. Chen, R. B. Wu, X. Q. Zhang, L. Wang, R. W. Jiang, W. C. Ye, *J. Nat. Prod.* **2017**, *80*, 1182–1186; c) R. R. Zhang, H. Y. Tian, Y. F. Tan, T. Y. Chung, X. H. Sun, X. Xia, W. C. Ye, D. A. Middleton, N. Fedosova, M. Esmann, J. T. Tzen, R. W. Jiang, *Org. Biomol. Chem.* **2014**, *12*, 8919–8929; d) S. Zhou, Q. Zheng, X. Huang, Y. Wang, S. Luo, R. Jiang, L. Wang, W. Ye, H. Tian, *Org. Biomol. Chem.* **2017**, *15*, 5609–5615.
- [8] Revolutionary Committee of Changchun College of Traditional Chinese Medicine. *Medicine, Jilin Chinese Herbal Medicine*, Jilin People's Press, Changchun, **1970**, pp. 754.
- [9] M. Graff, P. C. F. Buchholz, P. Stockinger, B. Bommarius, A. S. Bommarius, J. Pleiss, *Proteins* **2019**, *87*, 443–451.
- [10] X. F. Huang, V. Luu-The, *J. Biol. Chem.* **2000**, *275*, 29452–29457.
- [11] A. S. Devlin, M. A. Fischbach, *Nat. Chem. Biol.* **2015**, *11*, 685–689.
- [12] T. M. Penning, *Chem.-Biol. Interact.* **2015**, *234*, 236–246.
- [13] a) S. S. Smith, Q. H. Gong, F. C. Hsu, R. S. Markowitz, J. M. ffrench-Mullen, X. Li, *Nature* **1998**, *392*, 926–930; b) A. E. Calogero, M. A. Palumbo, A. M. Bosboom, N. Burrello, E. Ferrara, G. Palumbo, F. Petraglia, R. D'Agata, *J. Endocrinol.* **1998**, *158*, 121–125.
- [14] H. J. Tang, L. J. Ruan, H. Y. Tian, G. P. Liang, W. C. Ye, E. Hughes, M. Esmann, N. U. Fedosova, T. Y. Chung, J. T. C. Tzen, R. W. Jiang, D. A. Middleton, *Sci. Rep.* **2016**, *6*, 29155.

Manuscript received: August 15, 2022

Revised manuscript received: September 19, 2022

Accepted manuscript online: September 20, 2022

Version of record online: October 18, 2022